Cell Metabolism
Article

The Inflammasome-Mediated Caspase-1 Activation Controls Adipocyte Differentiation and Insulin Sensitivity

Rinke Stienstra,[1,*] Leo A.B. Joosten,[1,6] Tim Koenen,[1] Berry van Tits,[1] Janna A. van Diepen,[9] Sjoerd A.A. van den Berg,[10] Patrick C.N. Rensen,[9] Peter J. Voshol,[9] Giamilla Fantuzzi,[3] Anneke Hijmans,[1] Sander Kersten,[4,5] Michael Müller,[4,5] Wim B. van den Berg,[6] Nico van Rooijen,[7] Martin Wabitsch,[8] Bart-Jan Kullberg,[1] Jos W.M. van der Meer,[1] Thirumala Kanneganti,[2] Cees J. Tack,[1] and Mihai G. Netea[1]

[1]Department of Medicine, Radboud University Nijmegen Medical Centre and Nijmegen Institute for Infection, Inflammation and Immunity (N4I), Nijmegen 6525 GA, The Netherlands
[2]Department of Immunology, St. Jude Children's Research Hospital, Memphis, TN 38105, USA
[3]Department of Kinesiology and Nutrition, University of Illinois at Chicago, Chicago, IL 60612, USA
[4]Nutrition, Metabolism, and Genomics Group, Division of Human Nutrition, Wageningen University, Wageningen 6703 HD, The Netherlands
[5]Nutrigenomics Consortium, TI Food and Nutrition, Wageningen 6709 PA, The Netherlands
[6]Rheumatology Research and Advanced Therapeutics, Department of Rheumatology, Radboud University Nijmegen Medical Centre, Nijmegen 6525 GA, The Netherlands
[7]Department of Molecular Cell Biology, Vrije Universiteit Medical Center, Amsterdam 1081 BT, The Netherlands
[8]Division of Pediatric Endocrinology and Diabetes, University of Ulm, Ulm 89075, Germany
[9]Department of General Internal Medicine, Endocrinology, and Metabolic Diseases
[10]Department of Human Genetics
Leiden University Medical Center, Leiden 2333 ZA, The Netherlands
*Correspondence: r.stienstra@aig.umcn.nl
DOI 10.1016/j.cmet.2010.11.011

SUMMARY

Obesity-induced inflammation originating from expanding adipose tissue interferes with insulin sensitivity. Important metabolic effects have been recently attributed to IL-1β and IL-18, two members of the IL-1 family of cytokines. Processing of IL-1β and IL-18 requires cleavage by caspase-1, a cysteine protease regulated by a protein complex called the inflammasome. We demonstrate that the inflammasome/caspase-1 governs adipocyte differentiation and insulin sensitivity. Caspase-1 is upregulated during adipocyte differentiation and directs adipocytes toward a more insulin-resistant phenotype. Treatment of differentiating adipocytes with recombinant IL-1β and IL-18, or blocking their effects by inhibitors, reveals that the effects of caspase-1 on adipocyte differentiation are largely conveyed by IL-1β. Caspase-1 and IL-1β activity in adipose tissue is increased both in diet-induced and genetically induced obese animal models. Conversely, mice deficient in caspase-1 are more insulin sensitive as compared to wild-type animals. In addition, differentiation of preadipocytes isolated from *caspase-1*$^{-/-}$ or *NLRP3*$^{-/-}$ mice resulted in more metabolically active fat cells. In vivo, treatment of obese mice with a caspase-1 inhibitor significantly increases their insulin sensitivity. Indirect calorimetry analysis revealed higher fat oxidation rates in *caspase-1*$^{-/-}$ animals. In conclusion, the inflammasome is an important regulator of adipocyte function and insulin sensitivity, and caspase-1 inhibition may represent a novel therapeutic target in clinical conditions associated with obesity and insulin resistance.

INTRODUCTION

The prevalence of obesity, an important risk factor for type 2 diabetes, hypertension, and hyperlipidemia, has reached epidemic proportions worldwide (Mokdad et al., 2001). Initially viewed as a tissue that merely stores energy, recently it has become evident that adipose tissue also releases hormone-like mediators named adipokines, and exerts effects reminiscent of an endocrine organ (Lago et al., 2007). During the development of obesity, the morphology and functional properties of adipose tissue change dramatically. In addition to adipocyte hypertrophy due to storage of increasing amounts of lipids, adipose tissue turns into an inflamed tissue characterized by macrophage infiltration and altered secretion of adipokines (Hotamisligil, 2006; Weisberg et al., 2003). Whereas the secretion of proinflammatory cytokines is enhanced, the production of insulin-sensitizing adipokines such as adiponectin is reduced. To date, many proinflammatory cytokines have been linked to the development of insulin resistance and type 2 diabetes, including TNFα and IL-6 (Hotamisligil, 2006; Guilherme et al., 2008). More recently, interest has grown into the role of the IL-1 family of cytokines and its prominent members IL-1β and IL-18. IL-1β is a proinflammatory cytokine with a role in the pathogenesis of type 1 diabetes through its toxic effects on β cells of the pancreas (Ohara-Imaizumi et al., 2004). It has been shown that treatment of type 2 diabetic patients with IL-1Ra, an antagonist of IL-1

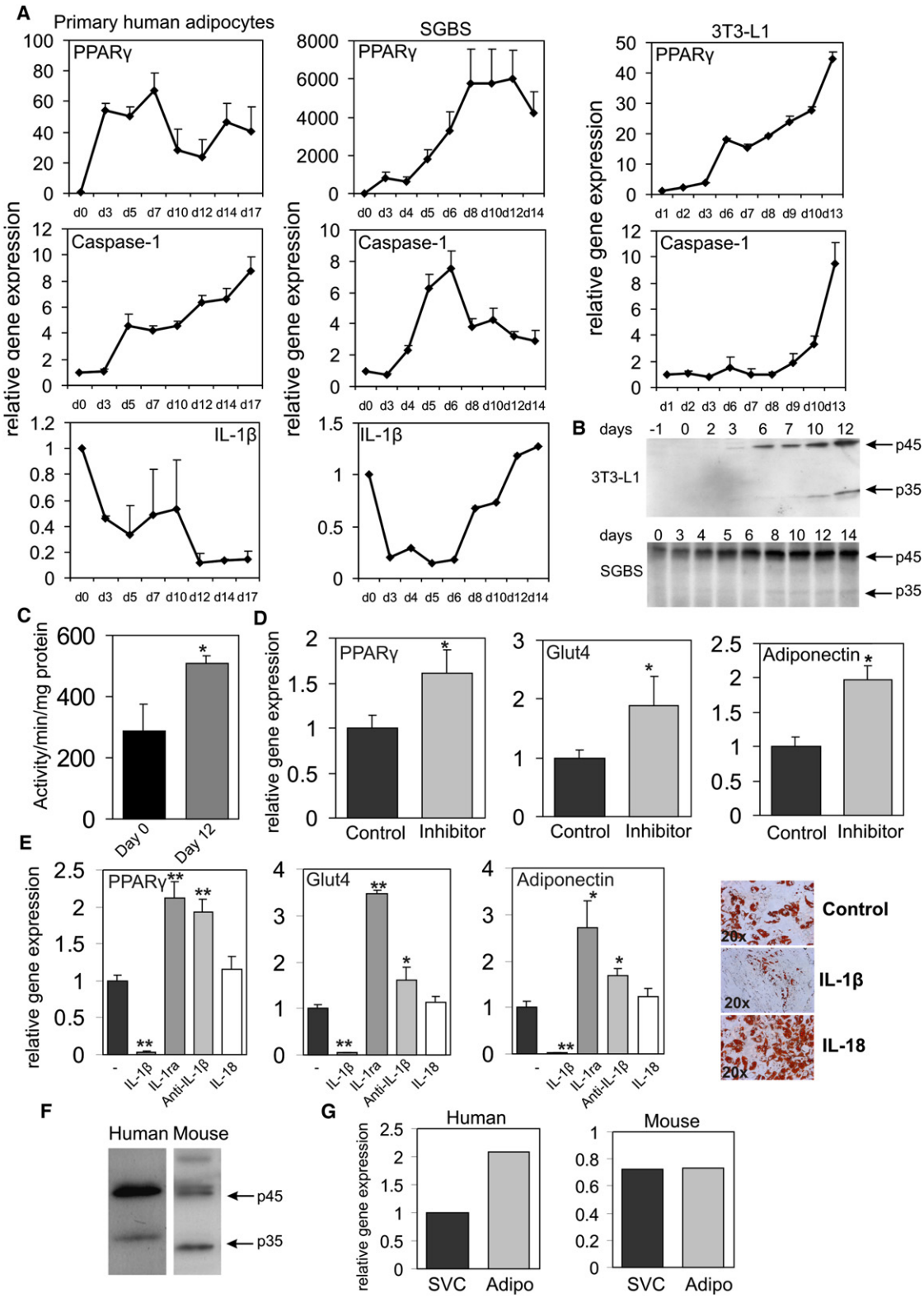

Figure 1. Caspase-1 Is Activated during Adipogenesis In Vitro and Is Present in Adipocytes of Mouse and Human White Adipose Tissue In Vivo

(A) Quantitative PCR analysis of differentiating human or mouse adipocytes. Representative results are shown of n = 3 experiments.

(B) Western blot analysis of caspase-1 protein levels in differentiating mouse 3T3-L1 adipocytes and human SGBS adipocytes. Protein marker is given in kDalton.

(C) Caspase-1 activity in preadipocytes (Pre) and adipocytes at day 8 of differentiation (Mature).

signaling, improves glycemic control and β cell function (Larsen et al., 2007). Recent work has also revealed an important role of IL-18 in modulation of energy balance and insulin sensitivity (Netea et al., 2006).

In order to be activated, IL-1β and IL-18 have to be processed from inactive precursors by an intracellular cysteine protease called caspase-1 (Petrilli et al., 2007; Wilmanski et al., 2008). Activation of caspase-1 itself takes place by conformational changes in a protein platform called the inflammasome, consisting of caspase-1 and proteins of the NACHT-LRR (NLR) family including NLRP3 and ASC, leading to the release of the active enzyme (Kanneganti et al., 2007). The inflammasome is activated in response to so-called danger-associated molecular patterns, which can be elicited either by microbial components (e.g., peptidoglycan) or by endogenous danger signals (e.g., uric acid, ATP) (Petrilli et al., 2007). Because of the metabolic effects described for IL-1β and IL-18, and due to the crucial role of caspase-1 for the activation of these cytokines, we hypothesized that inflammasome-dependent activation of caspase-1 plays an important role in the metabolic function of the adipose tissue. This hypothesis was tested using a number of in vitro and in vivo approaches.

RESULTS

Expression and Function of Caspase-1 in Adipocytes

To explore the role of the caspase-1 in adipocyte function, we first assessed the expression of caspase-1 during in vitro adipogenesis. Interestingly, differentiation of mouse 3T3-L1, human Simpson-Golabi-Behmel syndrome (SGBS), and human primary adipocytes was associated with a significant increase in expression of caspase-1 in parallel with the adipogenic transcription factor PPARγ (Figure 1A). IL-1β gene expression levels during adipocyte differentiation displayed a more variable pattern (Figure 1B).

Caspase-1 protein levels were significantly higher in differentiated cells (Figure 1B), and caspase-1 activity levels were increased in fully differentiated adipocytes versus preadipocytes (Figure 1C). In order to assess whether caspase-1 influences adipocyte differentiation, we blocked caspase-1 with the caspase-1 inhibitor Pralnacasan (Rudolphi et al., 2003). This inhibitor more effectively reduced caspase-1 activity compared to the frequently used caspase-1 inhibitor Yvad, as determined by an in vitro caspase-1 activity assay (see Figure S1A available online). Caspase-1 blockade improved expression levels of adipogenic marker genes including PPARγ, adiponectin, and Glut4 gene expression (Figure 1D). Importantly, caspase-1 blockage in human adipose tissue using Pralnacasan reduced the secretion of IL-1β (Figure S1B). In addition to caspase-1 inhibition using an inhibitor, caspase-1 function was silenced using siRNA. Treatment of cells with siRNA targeted to caspase-1 led to a significant reduction in caspase-1 gene expression (relative gene expression levels, 1.00 ± 0.04 versus 0.16 ± 0.01). In addition to mRNA levels, caspase-1 protein levels were decreased in cells transected with siRNA targeted against caspase-1 (Figure S2A). Basal secretion levels of bioactive IL-1, as measured by using the murine thymoma cell line EL4/NOB 1 that produces IL-2 in response to bioactive IL-1, were unchanged in cells depleted of caspase-1. Probably, levels of IL-1 produced by the cells under normal conditions are relatively low, and the secreted IL-1 may directly bind to the cell membrane. Silencing of caspase-1 in SGBS adipocytes improved insulin sensitivity as determined by pAKT/AKT ratios after short-term insulin treatment (mock versus siRNA caspase-1, 0.95 ± 0.14 versus 2.10 ± 0.16; p value < 0.005). Finally, treatment of caspase-1-depleted cells with recombinant IL-1β led to a reduction in pAKT levels (Figure S2B).

To examine whether the effects of caspase-1 may be mediated by processing of IL-1β or IL-18, we studied the effects of these cytokines on adipocyte differentiation. Whereas recombinant IL-1β blocked adipogenesis, as assessed by oil red O staining, recombinant IL-18 had no affect (Figure 1E). Importantly, treatment of differentiating adipocytes with recombinant IL-1 receptor antagonist to block endogenous IL-1 signaling mirrored the effects of caspase-1 inhibition (Figure 1E). Moreover, specific blockage of IL-1β-signaling pathways in differentiating SGBS adipocytes using an anti-IL-1β antibody also resulted in an improvement of adipogenesis (Figure 1E). Thus, effects of caspase-1 on adipogenesis are likely conveyed via endogenous IL-1β. In order to confirm that caspase-1 has a functional role in vivo, caspase-1 protein levels were assessed in human and mouse white adipose tissue. Both human and mouse white adipose tissue displayed total (45 kDA) and activated caspase-1 isoforms (34 kDA) (Figure 1F). Fractioning of total human and mouse white adipose tissue into mature adipocytes and stromal vascular cells revealed that caspase-1 is expressed in both cell populations (Figure 1G). Taken together, our data show that caspase-1 is upregulated during in vitro adipocyte differentiation and is present in mouse and human white adipose tissue in vivo.

Caspase-1 Function in Experimental Models of Obesity

To determine caspase-1 function in adipose tissue during diet-induced obesity, C57Bl/6 mice were fed a high-fat diet (HFD) for 16 weeks. HFD feeding caused obesity, as illustrated by increased bodyweight (Figure 2A) and epididymal adipose tissue mass (Figure 2B). Importantly, after prolonged HFD, adipose tissue expression of caspase-1 was markedly increased (Figure 2C). A similar increase in caspase-1 mRNA and protein was observed in obese db/db mice and ob/ob mice (Figure 2D). Protein levels of the active isoform of caspase-1 (34 kDA) were increased in white adipose tissue of obese animals (Figure 2E). Noticeably, specificity of the antibody used to detect caspase-1 protein levels was tested by using adipose tissue of wild-type and

(D) Quantitative PCR analysis of SGBS adipocytes differentiated for 12 days in the presence of the specific caspase-1 inhibitor Pralnacasan at 100 μM.
(E) Quantitative PCR analysis and representative oil red O staining of SGBS adipocytes differentiated for 7 days in the presence of recombinant IL-1β (10 ng/ml), IL-1ra (5 μg/ml), anti-IL-1β antibody (5 μg/ml), or IL-18 (25 ng/ml).
(F) Western blot analysis of caspase-1 in total human and mouse white adipose tissue. Protein marker is given in kDalton.
(G) Caspase-1 expression in the stromal vascular cells and mature adipocytes fractionated from total white adipose tissue. Data are presented as mean ± SEM. Asterisks depict statistically significant differences between control and experimental groups. *p < 0.05, **p < 0.005.

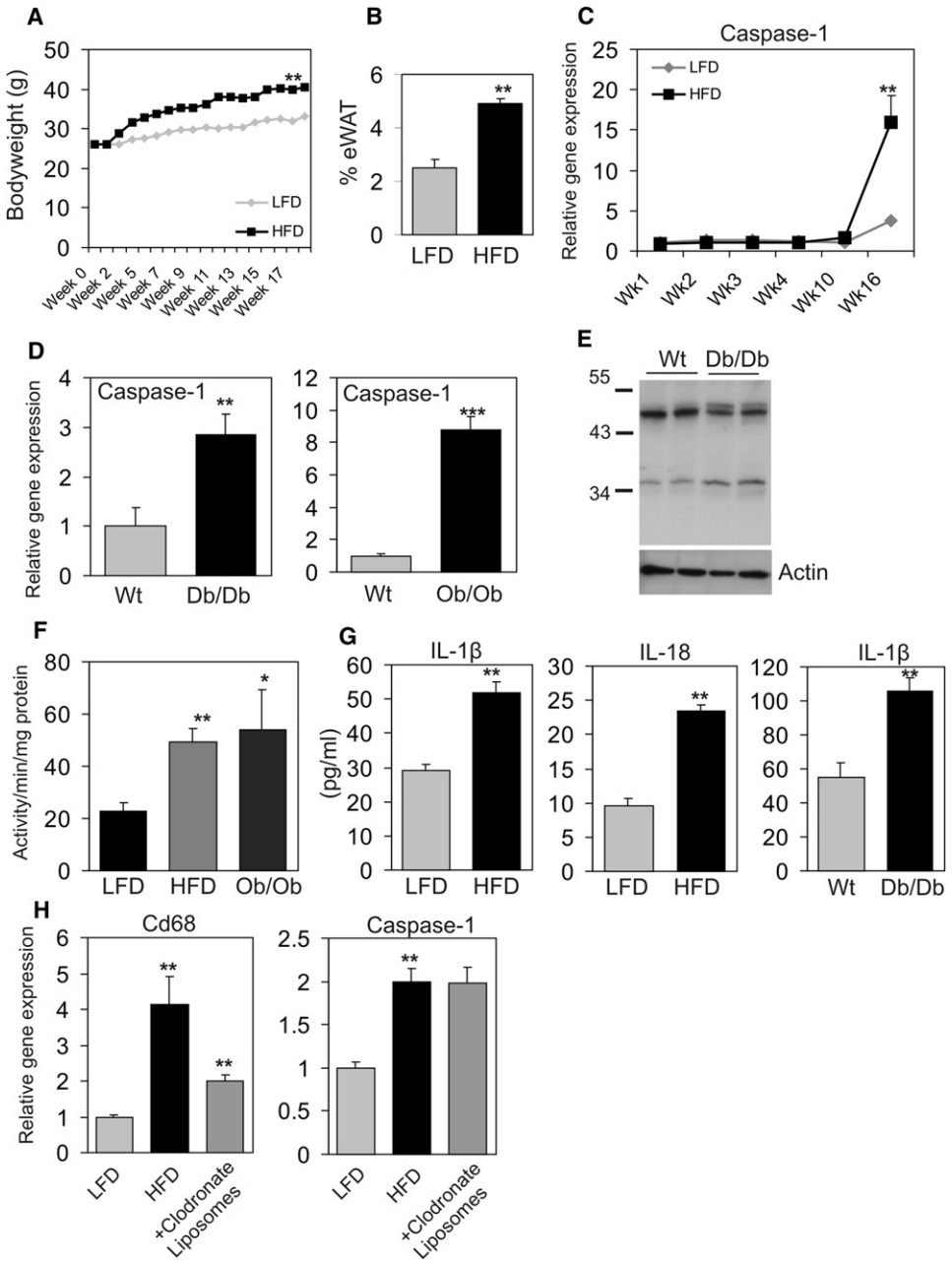

Figure 2. Caspase-1 Is Activated in Adipocytes of Diet-Induced and Genetically Induced Obese Animals

(A) Bodyweight development in male wild-type C57/bl6 animals (2 months of age at start of intervention) fed either a LFD or HFD (n = 10 per group).

(B) Percent of epididymal white adipose tissue after 17 weeks of HFD feeding.

(C) Quantitative PCR analysis of caspase-1 gene expression in white adipose tissue of C57/Bl6 animals during dietary intervention (n = 6 per group).

(D) White adipose tissue of wild-type, db/db, and ob/ob animals (4 months of age) is analyzed for caspase-1 gene expression levels using quantitative PCR analysis (n = 5 per group).

(E) Western blot analysis of caspase-1 in white adipose tissue of WT and db/db animals. Actin levels are shown as loading control.

(F) Caspase-1 activity levels measured in total white adipose tissue of LFD- or HFD-fed animals and ob/ob mice.

(G) IL-1β and IL-18 concentrations (pg/ml) measured in total white adipose tissue of WT animals fed a LFD or HFD and IL-1β concentrations (pg/ml) present in white adipose tissue of WT and db/db mice (n = 5 per group).

(H) Gene expression levels of CD68 and caspase-1 in white adipose tissue of wild-type animals (2 months of age at start of intervention) fed a LFD or a HFD for 16 weeks and a HFD followed by intraperitoneal injection with clodronate liposomes. Data are presented as mean ± SEM. Asterisks depict statistically significant differences between control and experimental groups. *$p < 0.05$, **$p < 0.005$, ***$p < 0.001$.

caspase-1$^{-/-}$ animals (Figure S3). In line with elevated gene expression and protein levels, caspase-1 activity was also increased in total white adipose tissue of HFD and ob/ob animals compared to lean mice (Figure 2F). The increased caspase-1 activity was accompanied by significantly elevated IL-1β and IL-18 protein levels in adipose tissue of diet-induced and genetically induced obese mice (Figure 2G). Although IL-1β and IL-18 protein levels were elevated, we were unable to detect any significant changes in gene expression of IL-1β and IL-18 in total adipose tissue of obese versus lean animals.

Previous studies have shown that obesity and adipocyte hypertrophy result in an influx of macrophages into adipose tissue (Weisberg et al., 2003; Xu et al., 2003), and we assessed whether the increased expression of caspase-1 in adipose tissue was due to an increase in the infiltrating macrophages or the adipocytes themselves. Partial depletion of macrophages from adipose tissue of animals fed a HFD decreased the expression of the macrophage marker CD68, yet did not alter the expression of caspase-1 (Figure 2H), suggesting that caspase-1 effects on adipose tissue are not only exerted through infiltrating macrophages. Together, these data show that both diet-induced and genetically induced obesity result in activation of caspase-1 and increased levels of IL-1β and IL-18 in adipose tissue.

Caspase-1 Modulates Adipocyte Function

To assess in more detail the role of caspase-1 in adipocyte function, preadipocytes from caspase-1-deficient mice and wild-type mice were differentiated toward adipocytes using a standard adipocyte differentiation protocol. In the absence of caspase-1, adipogenesis was enhanced, as illustrated by oil red O staining (Figure 3A) and increased gene expression levels of GLUT-4, adiponectin, and PPARγ (Figure 3B). Importantly, secretion of adiponectin, a key regulator of insulin sensitivity (Kadowaki et al., 2006), was significantly elevated in caspase-1-deficient adipocytes (Figure 3C). Additionally, insulin signaling in caspase-1-deficient adipocytes was ameliorated, as visualized by an increased phosphorylation of Akt (Figure 3D) (relative pAKT/AKT ratio, WT 10 nm insulin versus *caspase-1*$^{-/-}$ 10 nm insulin, 1 ± 0.53 versus 3.09 ± 0.12, p value < 0.05; WT 100 nm insulin versus *caspase-1*$^{-/-}$ 100 nm insulin, 4.13 ± 1.33 versus 8.85 ± 1.8, p value < 0.05). Importantly, in mature human adipocytes made insulin resistant by overnight treatment with 200 nM of insulin, caspase-1 inhibition increased insulin action as determined by pAKT levels after 20 min of insulin treatment (50 nM) (Figure 3E) (relative pAKT/AKT ratio, control versus inhibitor, 1 ± 0.24 versus 2.41 ± 0.15, p value < 0.01).

Because NLRP3 is an important component of the inflammasome involved in the activation of caspase-1 (Petrilli et al., 2007), we investigated whether absence of NLRP3 mimics the effects seen in caspase-1-deficient animals. Adipocyte differentiation of preadipocytes isolated from NLRP3-deficient animals was similarly enhanced compared to caspase-1-deficient cells (Figures 3F and 3G). Finally, we tested insulin sensitivity of total white adipose in wild-type, *caspase-1*$^{-/-}$, and *NLRP3*$^{-/-}$ animals. As shown in Figure 3H, the absence of caspase-1 and NLRP3 in white adipose tissue resulted in an increase in adipose tissue insulin sensitivity as determined by phosphorylation of AKT (relative pAKT/AKT ratio, WT versus *caspase-1*$^{-/-}$ versus *NALP3*$^{-/-}$, 10 nM insulin, 4.06 ± 0.54 versus 11.20 ± 1.66 versus 12.11 ± 2.19, p value < 0.05; 100 nm insulin, 5.56 ± 0.43 versus 14.47 ± 2.88 versus 29.23 ± 7.28, p value < 0.05) . In line with the rise in insulin sensitivity, IL-1β production of adipose tissue isolated from *caspase-1*$^{-/-}$ and *NLRP3*$^{-/-}$ animals was significantly reduced as compared to white adipose tissue from wild-type mice (Figure 3I). These data establish an important function of caspase-1 and NLRP3 in adipocyte formation and insulin sensitivity.

Absence of Caspase-1 Improves Insulin Sensitivity In Vivo

To unveil the potential role of caspase-1 in vivo, adipose tissue function and morphology were analyzed in caspase-1-deficient animals. The absence of caspase-1 led to a profound change in adipose tissue morphology (Figure 4A) with markedly smaller adipocytes (average adipocyte size, WT mice 966.8 μM^2, *caspase-1*$^{-/-}$ mice 629.16 μM^2, p value < 0.001) (Figure 4A). In addition, although total bodyweight was not different between both genotypes (Figure 4B), DEXA scan analysis of *caspase-1*$^{-/-}$ animals revealed a profound reduction in total fat mass (Figure 4B). On the other hand, bone mineral content was significantly elevated in *caspase-1*$^{-/-}$ animals compared to wild-type mice (Figure 4B).

In line with the beneficial change in adipose tissue morphology, gene expression analysis revealed elevated levels of PPARγ, adiponectin, and GLUT4, consistent with increased insulin sensitivity and improved glucose uptake in adipose tissue (Figure 4C). In addition, adipose PGC1α and PGC1β gene expression levels were highly elevated in caspase-1-deficient animals (Figure 4C), implying an increase in mitochondrial activity and energy expenditure (Handschin and Spiegelman, 2006). Indeed, quantification of mitochondrial DNA content in WAT of wild-type and *caspase-1*$^{-/-}$ animals revealed a robust increase in mtDNA of white adipose tissue in the absence of caspase-1 (Figure 4D).

Finally, our in vitro observations showing enhanced insulin action in caspase-1-deficient adipocytes were accompanied by an improvement in total insulin sensitivity in caspase-1-deficient animals, as illustrated by a decrease in basal plasma insulin levels and lower plasma glucose levels during insulin tolerance tests (Figures 4E and 4F). Assessment of whole-body insulin resistance by euglycemic hyperinsulinemic clamp analysis revealed a significant improvement of insulin sensitivity in *caspase-1*$^{-/-}$ animals as compared to wild-type mice (Figure 4G, Figure S4A, Table S1). Furthermore, both basal and hyperinsulinemic FFA concentrations were significantly lower in *caspase-1*$^{-/-}$ mice compared to control mice (basal, 0.69 ± 0.06 versus 0.89 ± 0.04, p value = 0.001; hyperinsulinemic, 0.30 ± 0.02 versus 0.41 ± 0.04, p value = 0.01), consistent with a reduction in lipolytic activity and an increase in insulin sensitivity of white adipose tissue in the absence of caspase-1. Other basal plasma lipids including triglycerides and cholesterol were not altered in caspase-1-deficient animals (data not shown). Since caspase-1 controls IL-1β activity, insulin tolerance was also analyzed in IL-1β-deficient animals. Insulin sensitivity was improved in IL-1β-deficient animals when compared to wild-type mice (Figure 4G). Finally, in line with the important role of NLRP3 in the activation of caspase-1, *NLRP3*$^{-/-}$ animals were more insulin sensitive compared to wild-type animals (Figure 4H). Noticeably, adipose tissue morphology in IL-1- and NLRP3-deficient animals was unchanged. Nevertheless,

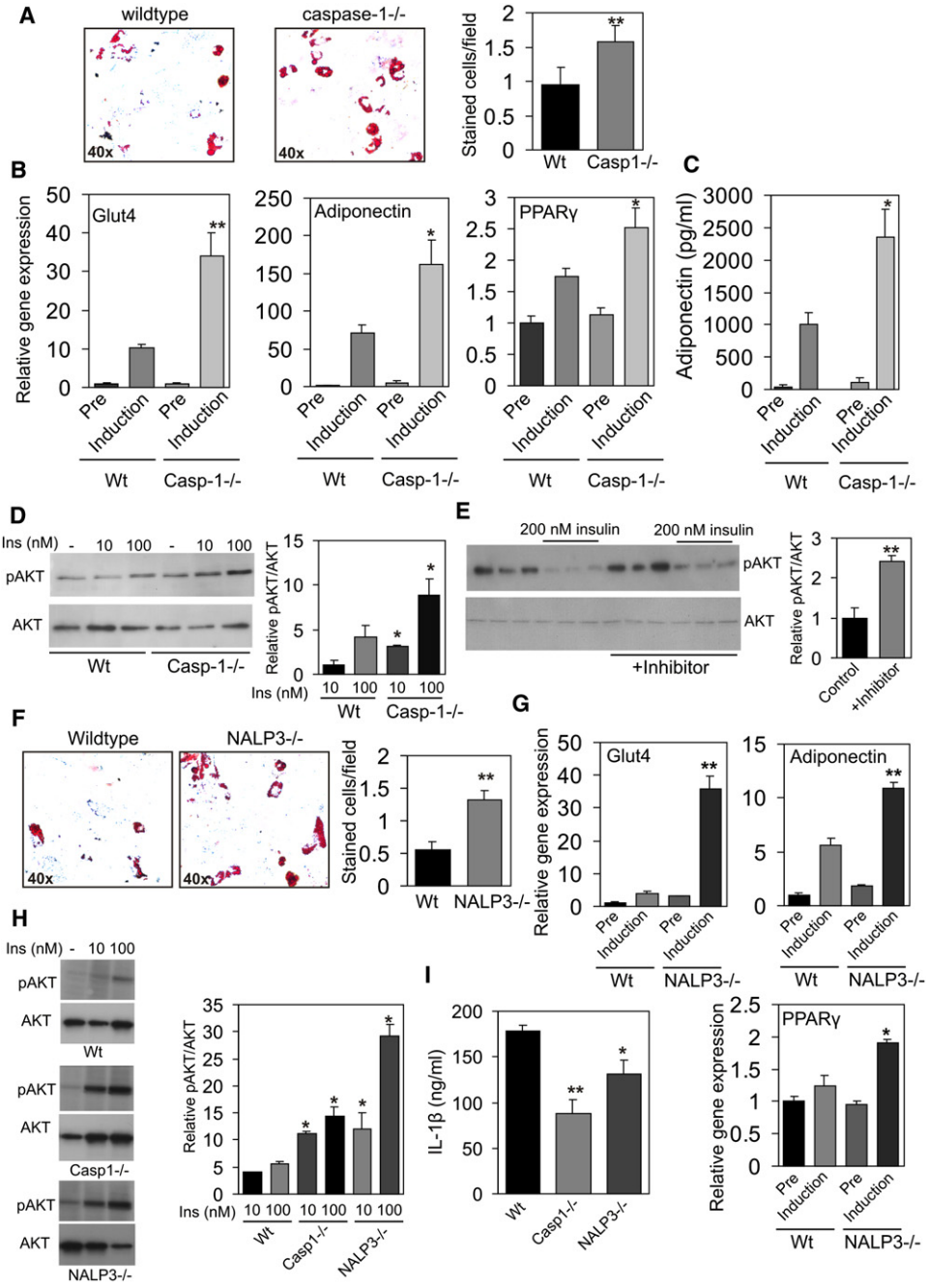

Figure 3. Absence of Caspase-1 and NLRP3 Improves Adipogenesis and Insulin Sensitivity in Differentiated Adipocytes

(A) Representative oil red O staining pictures and quantification of WT and caspase-1-deficient preadipocytes differentiated toward adipocytes for 7 days.

(B) GLUT4, adiponectin, and PPARγ gene expression levels as determined by quantitative real-time PCR in preadipocytes (Pre) or differentiated adipocytes (Induction) from WT or caspase-1-deficient animals.

(C) Adiponectin concentrations (pg/ml) measured in medium of preadipocytes (Pre) or adipocytes (Induction) differentiated for 7 days from WT or caspase-1-deficient animals.

(D) Western blot analysis of phosphorylated AKT and total AKT levels after insulin treatment for 20 min in adipocytes differentiated for 7 days.

(E) Western blot analysis of phosphorylated AKT and total AKT levels after 20 min of insulin treatment in mature SGBS adipocytes pretreated overnight with 200 nM of insulin and/or the caspase-1 inhibitor pralnacasan (100 μM).

(F) Representative oil red O staining pictures and quantification of WT and NLRP3-deficient preadipocytes differentiated toward adipocytes for 7 days.

(G) GLUT4, Adiponectin, and PPARγ gene expression levels in preadipocytes (Pre) or differentiated adipocytes (Induction) from WT or NALP3-deficient animals.

(H) Western blot analysis of phosphorylated AKT and total AKT levels in white adipose tissue explants from wild-type, *caspase-1*$^{-/-}$, and *NLRP3*$^{-/-}$ animals (2 months of age) after 20 min of insulin treatment.

(I) IL-1β production of adipose tissue explants from WT, *caspase-1*$^{-/-}$, and *NLRP3*$^{-/-}$ animals after 24 hr of culturing. Data are presented as mean ± SEM. Asterisks depict statistically significant differences between control and experimental groups. *$p < 0.05$, **$p < 0.005$.

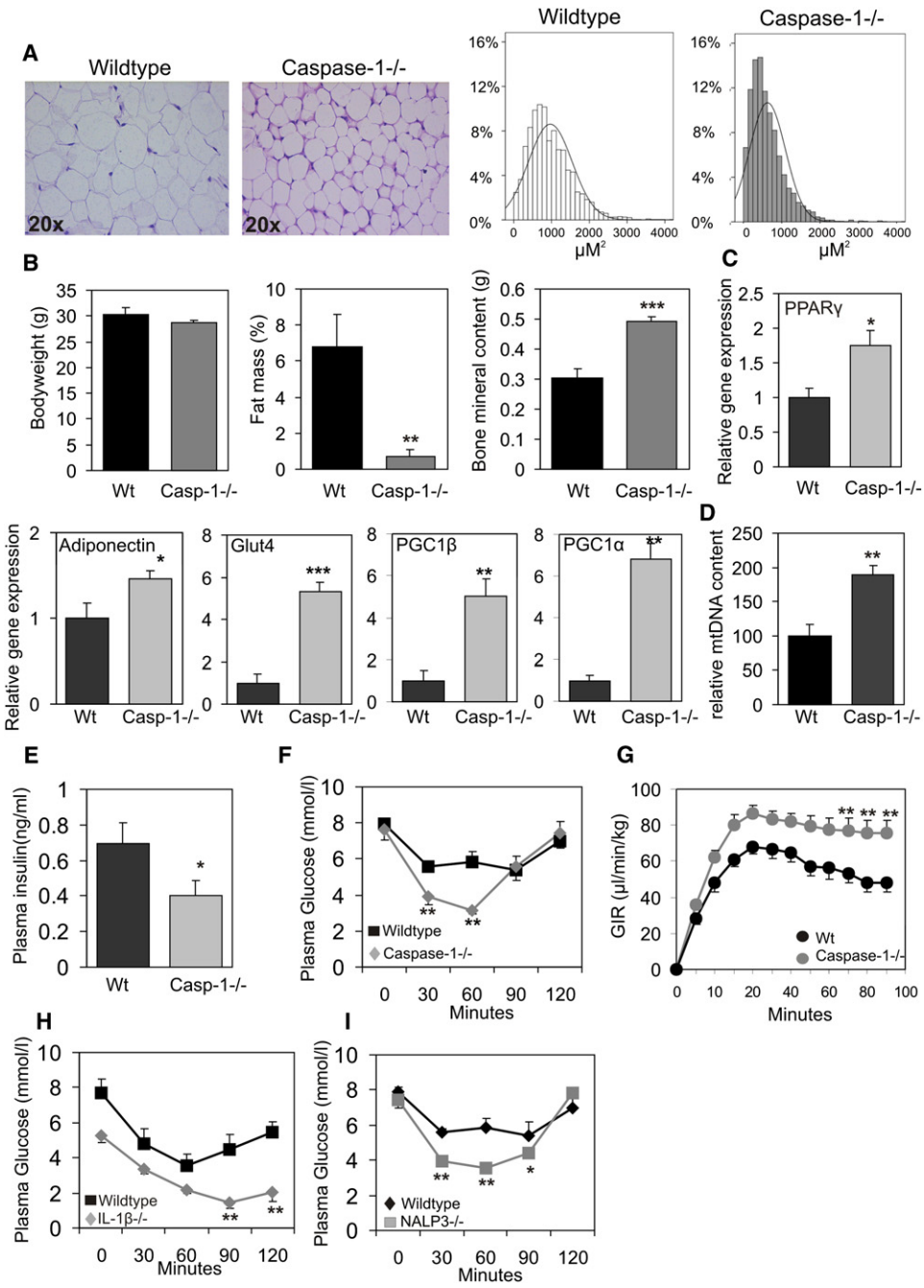

Figure 4. Caspase-1 Contributes to Adipose Tissue Formation and Function In Vivo

(A) Representative HE staining of white adipose tissue and quantification of adipocyte size.

(B) Total bodyweight, percentage of fat mass, and bone mineral content of WT and *caspase-1*$^{-/-}$ mice (6 months of age).

(C) Gene expression analysis of total white adipose of WT and caspase-1-deficient mice using real-time quantitative PCR techniques.

(D) mtDNA content of total white adipose tissue from WT and *caspase-1*$^{-/-}$ animals.

(E) Plasma insulin levels in nonfasted WT and caspase-1-deficient animals (n = 9 per group).

(F) Insulin tolerance test in WT and caspase-1-deficient animals (n = 9 per group).

(G) Assessment of whole-body insulin resistance by euglycemic hyperinsulinemic clamp analysis in wild-type (n = 17) and *caspase-1*$^{-/-}$ (n = 18) animals at 1 year of age. Glucose infusion rates (GIR) during the euglycemic hyperinsulinemic clamp analysis are shown.

(H) Insulin tolerance test in WT and IL-1β-deficient animals (n = 5 per group).

(I) Insulin tolerance test in WT and NALP3-deficient animals (n = 5 per group). Data are presented as mean ± SEM. Asterisks depict statistically significant differences between control and experimental groups. *p < 0.05, **p < 0.005, ***p < 0.001.

mtDNA content tended to be higher in *NLRP3*$^{-/-}$ animals, although differences were not statistically significant (Figure S4B).

Caspase-1 Inhibition during Obesity Improves Insulin Sensitivity

The involvement of caspase-1 in the modulation of insulin resistance renders it an attractive therapeutic target in clinical conditions such as type 2 diabetes. In order to provide the proof of principle that caspase-1 inhibition can improve insulin sensitivity, ob/ob mice were treated with a chemical inhibitor of caspase-1 activity. Animals orally received 200 mg/kg bodyweight caspase-1 inhibitor (Pralnacasan) or vehicle daily for 2 weeks. After 2 weeks of treatment, insulin tolerance tests were performed. Animals treated with the caspase-1 inhibitor showed a robust improvement of insulin sensitivity as compared to animals receiving vehicle only (Figure 5A). The effectiveness of caspase-1 inhibition was analyzed by measuring IL-1β protein levels in white adipose tissue. As expected, caspase-1 inhibition led to a significant reduction of IL-1β protein concentration in fat (Figure 5B). Noticeably, treatment of ob/ob animals with pralnacasan did not result in changes in fecal fat content or physical activity levels of the animals.

Interestingly, the improvement of insulin sensitivity was accompanied by an attenuated increase in bodyweight in animals receiving the caspase-1 inhibitor (Figure 5C), despite a similar daily food intake (Figure 5D). The percentage of epididymal white adipose tissue in ob/ob animals receiving the inhibitor tended to be lower as compared to animals receiving vehicle only (p value = 0.06), suggestive of changes in lipid storage and lipogenesis in white adipose tissue (Figure 5E).

Because lipid composition may be involved in the effects of caspase-1 on adipose tissue, the general lipid composition of the white adipose tissue was analyzed. As shown in Figure 5F, the amounts of C16:0 (palmitic acid) and C18:0 (stearic acid) present in white adipose tissue were significantly higher in animals receiving the inhibitor, whereas the concentration of C18:1 (oleic acid) was lower. Finally, the ratios of C16:1/C16:0 and C18:1/C18:0, indicative of desaturation through SCD-1 activity, were lower in ob/ob animals treated with the inhibitor (Figure 5G), suggestive of a decrease in lipogenesis.

Inasmuch as no changes were observed in the ratios of C18:0/C16:0 and C16:1/C18:1 (data not shown), elongase activity appeared to be unchanged. Noticeably, fatty acid composition and ratios of C18:1/C18:0 and C16:1/C16:0 in plasma samples were unchanged. Plasma FFA levels were unchanged in ob/ob animals fed the inhibitor as compared to the control animals (0.18 mM ± 0.04 versus 0.18 mM ± 0.009).

The effect of caspase-1 on the development of obesity and insulin resistance was analyzed using a diet intervention. Ten weeks of HFD feeding led to significantly less bodyweight gain in *caspase-1*$^{-/-}$ mice as compared to HFD-fed wild-type animals (Figure 5H), despite a similar food intake (Figure 5I). Moreover, insulin sensitivity as measured by an ITT test was significantly higher in *caspase-1*$^{-/-}$ animals compared to wild-type mice fed the HFD (Figure 5J).

Absence of Caspase-1 Increases Fat Oxidation Rate

Inasmuch as the inhibition of caspase-1 attenuates bodyweight gain despite a similar food intake, *caspase-1*$^{-/-}$ and C57Bl/6 wild-type mice were subjected to indirect calorimetry analysis using metabolic cages to determine their energy expenditure. Food intake and respiratory gas exchange was measured at 7 min intervals for a period of 60 hr. Respiratory gas exchange was calculated from oxygen consumption and carbon dioxide production and analyzed separately for diurnal and nocturnal periods to distinguish between periods of low (diurnal) and high (nocturnal) physical activity.

In line with our previous results, food intake was similar in both groups (wild-type, 4.99 ± 0.26 g/day; *caspase-1*$^{-/-}$, 4.62 ± 0.15 g/day; p value = 0.3). Fecal output (wild-type, 1.4 ± 0.07 g/day; *caspase-1*$^{-/-}$, 1.4 ± 0.07 g/day; p value = 0.9) as well as fecal fat content (steatocrit percent, WT, 7.13 ± 0.38; *caspase-1*$^{-/-}$, 8.02 ± 0.49; p value = 0.17) were not different between both genotypes.

Total energy expenditure did not differ between groups during the nocturnal period (WT, 0.54 ± 0.03 kcal/hr; *caspase-1*$^{-/-}$, 0.62 ± 0.03 kcal/h; p value = 0.06), nor the diurnal period (WT, 0.45 ± 0.02 kcal/hr; *caspase-1*$^{-/-}$, 0.45 ± 0.02 kcal/hr; p value = 0.9). Interestingly, diurnal RER values were significantly lower in *caspase-1*$^{-/-}$ animals (WT, 0.919 ± 0.012; *caspase-1*$^{-/-}$, 0.885 ± 0.006) (Figure 6A). The lower RER values were translated into a higher absolute fat oxidation rate during the diurnal part of the day (WT, 0.09 ± 0.01 kcal/hr; *caspase-1*$^{-/-}$, 0.13 ± 0.01 kcal/hr; p value = 0.02) (Figure 6B). Nocturnal relative and absolute fat oxidation rates as well as total diurnal and nocturnal carbohydrate oxidation rates did not differ between groups (Figures 6B and 6C). Together, these data indicate that *caspase-1*$^{-/-}$ animals have higher fat oxidation rates compared to controls, while food intake and fecal output were equal between groups.

DISCUSSION

In the present study we demonstrate that during differentiation and lipid accumulation, adipose tissue undergoes important proinflammatory changes represented by inflammasome and caspase-1 activation. These changes lead to a higher level of IL-1β production and contribute to the induction of insulin resistance.

The importance of inflammation and infiltration of macrophages in the modulation of adipose tissue function and insulin resistance has been intensively studied over the last years (Hotamisligil, 2006; Weisberg et al., 2003). IL-1β has been previously linked to obesity-induced inflammation and the development of insulin resistance in adipose tissue (Jager et al., 2007; Lagathu et al., 2006). Our results demonstrate that caspase-1 activation in adipose tissue of obese animals takes place partly independent of macrophage infiltration, induces the release of IL-1β, and finally results in the development of insulin resistance through autocrine and paracrine effects. In the absence of caspase-1, adipocytes differentiate more efficiently and are more sensitive to insulin. We observed similar effects in the absence of the inflammasome component NLRP3 that has been previously demonstrated to mediate caspase-1 activation (Petrilli et al., 2007). In addition to robust changes in adipose tissue morphology, we also suggest that the absence of caspase-1 results in an increased mitochondrial energy dissipation reflected by an increase in PGC-1α and PGC-1β gene

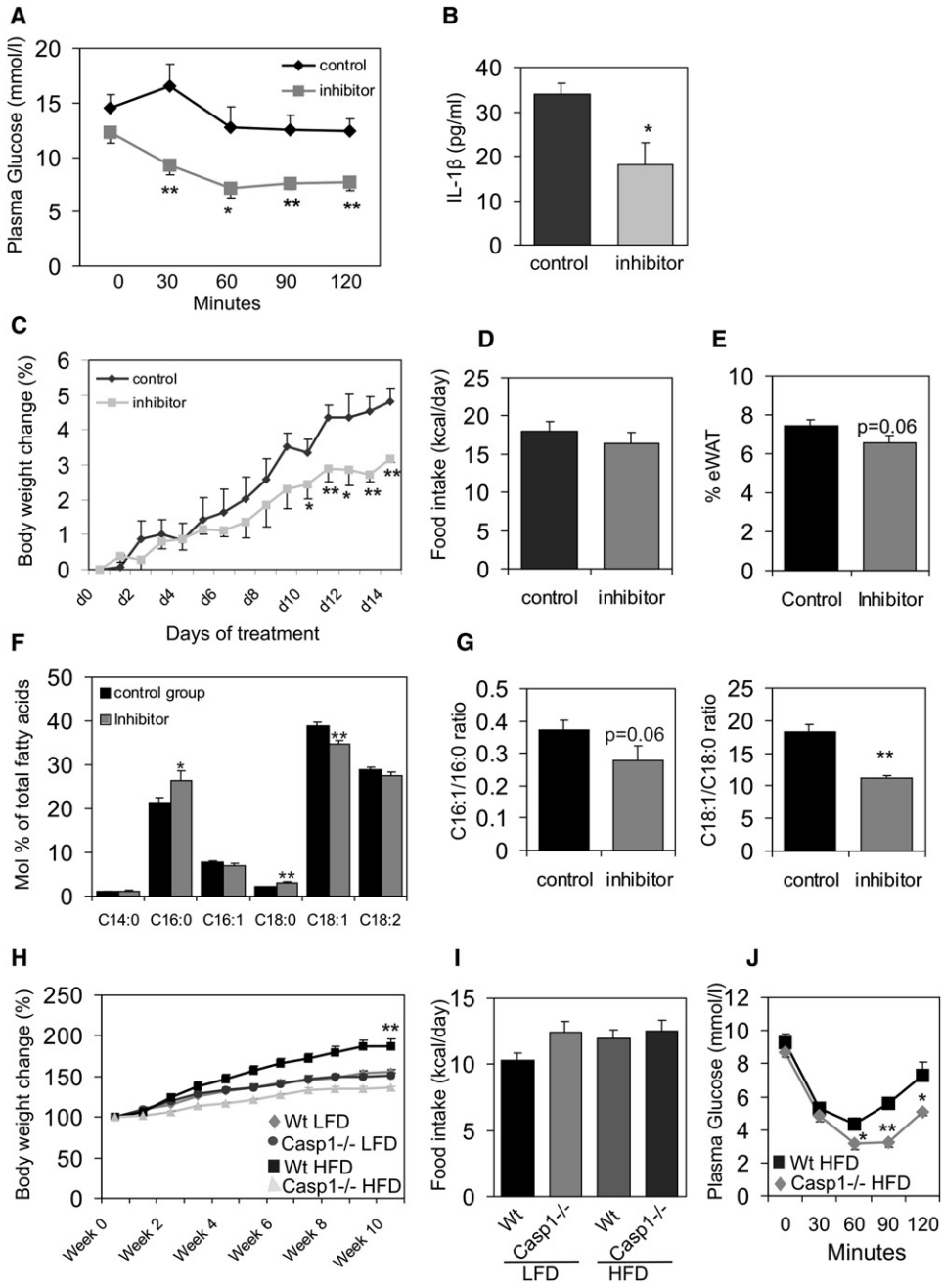

Figure 5. Caspase-1 Blockage Improves Insulin Sensitivity

(A) Insulin tolerance test in male ob/ob animals (2 months of age at start of intervention) orally treated with a chemical caspase-1 inhibitor (Pralnacasan) or vehicle for 2 weeks (n = 5 per group).

(B) IL-1β concentrations (pg/ml) measured in total white adipose tissue of ob/ob mice receiving vehicle or a caspase-1 inhibitor (n = 5 per group).

(C) Bodyweight change (in %) during oral treatment of ob/ob animals with vehicle or a caspase-1 inhibitor (n = 5 per group).

(D) Food intake (kcal/day) of ob/ob animals orally treated with a chemical caspase-1 inhibitor or vehicle for 2 weeks.

(E) Percentage of epididymal white adipose tissue.

(F) Lipid composition of white adipose tissue.

(G) Desaturation indexes in vehicle or caspase-1 inhibitor-treated animals.

(H) Bodyweight development of WT or *caspase-1*$^{-/-}$ animals (2 months of age at start of intervention) fed a LFD or HFD for 10 weeks (n = 10 per group).

(I) Food intake (kcal/day) of WT or *caspase-1*$^{-/-}$ fed a LFD or HFD.

(J) Insulin tolerance test in WT and *caspase-1*$^{-/-}$ animals fed a HFD for 10 weeks (n = 5 per group). Data are presented as mean ± SEM. Asterisks depict statistically significant differences between control and experimental groups.*$p < 0.05$, **$p < 0.005$.

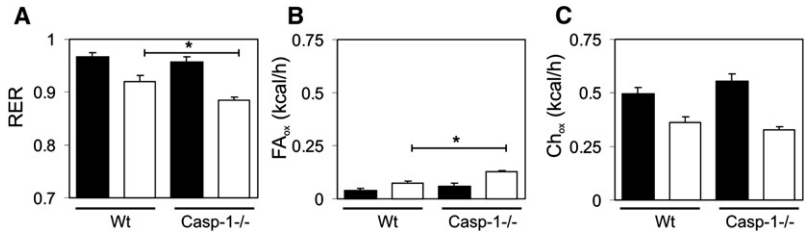

Figure 6. Absence of Caspase-1 Augments Fat Oxidation Rate

(A) Respiratory exchange rates, (B) fat oxidation, and (C) carbohydrate oxidation levels in WT and *caspase-1*$^{-/-}$ animals. Black and white bars represent mean nocturnal and diurnal data ± SEM, respectively. Asterisk indicates $p < 0.05$.

expression and enhancement of mtDNA content in white adipose tissue. Expression levels of PGC-1α and -β in caspase-1-deficient animals are probably increased due to the absence of bioactive IL-1β (Kim et al., 2007). Assessment of additional metabolic parameters of *caspase-1*$^{-/-}$ animals revealed that, although total caloric expenditure as well as food intake and fecal output did not differ between groups, absolute fat oxidation rates were higher in *caspase-1*$^{-/-}$ animals. Whereas fat oxidation comprised 20% of the total amount of diurnal caloric expenditure in wild-type animals, it contributed up to 30% in the *caspase-1*$^{-/-}$ animals. Ultimately, this results in a less positive fat balance and can explain the reduction in fat mass observed in *caspase-1*$^{-/-}$ animals.

In addition to activation of IL-1β, caspase-1 also cleaves pro-IL-18 to its bioactive form. In line with activation of caspase-1 in adipose tissue, IL-18 protein levels were increased in adipose tissue of HFD-fed animals compared to mice fed the LFD. However, our in vitro data show that the effects of IL-18 on adipocyte differentiation and gene expression are minor as compared to IL-1β. In addition, it has been previously shown that aging *IL-18*$^{-/-}$ animals develop obesity and insulin resistance (Netea et al., 2006). Overall this suggests that, although IL-1β and IL-18 both serve as substrates of caspase-1, the effects of these cytokines on adipocyte function and insulin sensitivity appear to be opposite, and the absence of IL-1β masks the effects of IL-18.

Importantly, we show that caspase-1-deficient animals are more insulin sensitive, which strongly supports the concept of the involvement of the inflammasome/caspase-1 pathway in the development of insulin resistance associated with obesity. Additionally, we demonstrate that blockage of caspase-1 in obese and insulin-resistant animals results in an improvement of insulin sensitivity and a smaller increase in total bodyweight. This reduction in weight gain is also reflected by a lower adipose tissue mass in animals receiving the caspase-1 inhibitor. The relatively small reduction in adipose tissue mass in animals receiving the inhibitor may be partly explained by the limited treatment period. Longer treatment of the animals with a caspase-1 inhibitor might lead to more pronounced differences in adipose tissue mass. In addition to the quantitative changes, we also observed qualitative changes in adipose tissue composition, illustrated by a significantly lower desaturation in white adipose tissue of animals treated with the inhibitor. This suggests that SCD-1 activity that catalyzes the synthesis of monounsaturated fatty acids is lower after caspase-1 inhibition. Since *SCD-1*$^{-/-}$ animals have a reduction in adiposity due to enhanced lipid oxidation together with an improvement in insulin sensitivity (Ntambi et al., 2002), regulation of SCD-1 activity by caspase-1 in adipose tissue may partly explain our observations. Inasmuch as SREBPs, which partly control SCD-1 activity, are processed and activated by caspase-1 (Gurcel et al., 2006), it may explain the reduction in desaturation index in adipose tissue of ob/ob animals after caspase-1 inhibition.

Hypothetically, the absence of caspase-1 in adipose tissue leads to an enhanced adipogenesis paralleled by an improvement in lipid oxidation due to enhanced mitochondrial function. The stimulation of adipogenesis in *caspase-1*$^{-/-}$ animals might primarily prevent lipid accumulation in non-fat tissues. In addition, it is unlikely that caspase-1 activation in adipose tissue will solely lead to IL-1β and IL-18 production, since it has been reported that caspase-1 is able to cleave additional substrates (Lamkanfi et al., 2008a). Adipocyte-specific proteins may also serve as caspase-1 substrates leading to functional changes in adipose tissue of obese animals. Interestingly, it has been shown that caspase-1 is able to cleave and inactivate PPARγ in adipocytes (He et al., 2008) that may also contribute to the detrimental effects of caspase-1 activation in adipose tissue of obese animals. Furthermore, adipose tissue-independent effects of caspase-1 may also contribute to the development of obesity-induced insulin resistance. Future studies are needed to resolve this issue and will shed more light on the mechanisms responsible for the resistance to diet-induced obesity in *caspase-1*$^{-/-}$ animals.

Beneficial effects of IL-1 blockade by the natural antagonist IL-1Ra have been recently reported in type 2 diabetes patients (Larsen et al., 2007), and our data provide the rationale for proposing caspase-1 inhibition as a potential novel therapeutic target in conditions associated with obesity and/or insulin resistance.

One important question that remains to be answered regards the precise mechanisms leading to caspase-1 activation during accumulation of fat in the adipocytes. It is still conceivable that the influx of macrophages might influence the activation of adipocyte-specific caspase-1, although our in vitro experiments showing caspase-1 activation in adipocytes in settings free of inflammatory cells suggest that adipocytes represent an important source of caspase-1. Nevertheless, our results do not rule out crosstalk between adipocyte-specific caspase-1 and production of IL-1β by macrophages in adipose tissue. Alternatively, lipids themselves or other mediators encountered in the obese patient (e.g., adipokines) could induce activation of caspase-1. Finally, glycemic conditions might induce caspase-1 activation in adipose tissue. Interestingly, hyperglycemic conditions have been shown to activate NLRP3 in pancreatic cells, and a similar mechanism may exist in adipose tissue (Zhou et al., 2010). Unraveling these molecular mechanisms is one of the important challenges for the near future.

In conclusion, our data reveal a novel metabolic function of the inflammasome/caspase-1 in adipose tissue. An increase in fat

mass causes upregulation and activation of caspase-1 that counteracts the normal metabolic function of adipose tissue leading to insulin resistance. Inhibition of caspase-1 in obese and insulin-resistant animals strongly improves insulin sensitivity together with changes in adipose tissue mass and composition. Importantly, the absence of caspase-1 results in an enhancement of overall fat oxidation rates. These findings suggest that pharmacological inhibition of caspase-1 in obese and/or patients with type 2 diabetes may restore the metabolic function of adipose tissue and subsequently improve insulin sensitivity.

EXPERIMENTAL PROCEDURES

Animal Studies

IL-1β$^{-/-}$ mice were a gift from J. Mudgett, Merck Research Laboratories, Rahway, USA. *Caspase-1*$^{-/-}$ mice were a kind gift from Prof. Dinarello, Department of Medicine, University of Colorado Health Sciences Center, Denver, CO 80262, USA. *NLRP3*$^{-/-}$ mice were generated as described previously (Kanneganti et al., 2006). All mice were backcrossed ten generations to C57Bl/6 mice, and age-matched wild-type C57Bl/6J mice were used as controls throughout the different experiments. Db/db and ob/ob mice in a C57Bl/6 background were obtained from the Jackson Laboratories.

Diet Intervention

Wild-type C57Bl/6J male mice received a LFD or a HFD for 16 weeks, providing 10% or 45% energy percent in the form of triglycerides (D12450B or D12451, Research Diets, New Brunswick, USA). In the last week of dietary intervention, some animals were injected intraperitoneally with clodronate liposomes. The liposomes were prepared as described previously (van Rooijen and Sanders, 1994) using phosphatidylcholine (Lipoid GmbH, Ludwigshafen, Germany) and cholesterol (Sigma Chem.Co. USA). Cl_2MDP (or clodronate) was a gift of Roche Diagnostics GmbH, Mannheim, Germany. *Caspase-1*$^{-/-}$ and wild-type mice were fed the similar LFD or HFD during 10 weeks. Insulin-tolerance tests were performed as previously described (Miyake et al., 2002). Briefly, animals were fasted for 4 hr and insulin was given intraperitoneally at a dose of 0.75 U/kg bodyweight. Blood samples were taken before and 30, 60, 90, or 120 min after insulin administration. Plasma levels of insulin and adiponectin secretion in cell culture medium were measured using ELISA (LINCO Research Inc., St. Charles, MO, USA).

Euglycemic Hyperinsulinemic Clamp Analysis

Euglycemic hyperinsulinemic clamps were performed as described earlier (Voshol et al., 2001). Briefly, after an overnight fast, animals were anesthetized with 6.25 mg/kg acepromazine (Sanofi Santé Nutrition Animale, Libourne Cedex, France), 6.25 mg/kg midazolam (Roche, Mijdrecht, The Netherlands), and 312.5 μg/kg fentanyl (Janssen-Cilag, Tilburg, the Netherlands), and an infusion needle was placed in the tail vein. A bolus of insulin (3 mU) was given, and a hyperinsulinemic euglycemic clamp was started with a continuous infusion of insulin (5 mU/h) and a variable infusion of 12.5% D-glucose (in PBS) to maintain blood glucose level at euglycemic levels. Blood samples were taken every 5–10 min from the tip of the tail to monitor plasma glucose levels (AccuCheck). Seventy, eighty, and ninety minutes after the start of the clamp, blood samples (70 μl) were taken for determination of plasma glucose, insulin, and FFA concentrations. Plasma glucose, insulin, and FFA levels were determined using commercially available kits (Instruchemie; Crystal Chem, Inc.; and Wako Pure Chemical Industries, respectively).

Indirect Calorimetry

Animals were housed in a controlled environment (23°C, 55% humidity) under a 12 hr light-dark cycle (07:00–19:00). Food and tap water were available ad libitum during the whole experiment. Mice were fed normal laboratory chow (RM3, Special Diet Services, UK) throughout the experiment. Indirect calorimetry was performed for a period of 60 hr (Comprehensive Laboratory Animal Monitoring System, Columbus Instruments, Columbus, OH, US). An acclimatization period of 24 hr prior to the start of the experiment was included. Food intake, oxygen consumption (VO_2), and carbon dioxide production rates (VCO_2) were measured at intervals of 7 min. Respiratory exchange ratio (RER) was calculated as the ratio between VCO_2 and VO_2. Absolute oxidation rates for fat and carbohydrate were calculated according to Peronnet and Massicotte (Peronnet and Massicotte, 1991). Fecal output was determined at the end of the experiment. Fat content of the feces was analyzed using the acid steatocrit method as described previously (Dumasy et al., 2004).

All the animal studies were approved by the animal experimentation committees of Wageningen University; Leiden University Medical Center and Radboud University Nijmegen Medical Centre, the Netherlands; the University of Illinois at Chicago, Chicago, IL, USA; and St. Jude Children's Research Hospital, Memphis, TN, USA.

IL-1β and IL-18 Measurements

IL-1β concentrations in white adipose tissue or cell culture medium were determined using a specific radioimmunoassay as previously described (Netea et al., 1996). IL-18 concentrations in white adipose tissue were measured using a commercially available ELISA (Invitrogen). Bioactive IL-1 was measured using the murine thymoma cell line EL4/NOB 1 that produces IL-2 in response to bioactive IL-1 (Netea et al., 1999). IL-2 levels were subsequently measured by ELISA (R&D).

Cell Culture

Mouse 3T3-L1 cells and human SGBS cells were cultured and differentiated toward adipocytes as described previously (Stienstra et al., 2008; Wabitsch et al., 2001). Oil red O staining of cells was performed using a standard protocol. Oil red O staining was quantified by using total photographic images of the staining which were divided in multiple fields, and the number of positive cells per field were counted. Two hours before insulin treatment of cells to assess insulin sensitivity, cells were cultured in serum-free medium.

Caspase-1 Activity Assay

Caspase-1 activity was measured in isolated adipocytes and total white adipose tissue using a fluorometric assay (Biovision, CA, USA) following the manufacturer's instructions with slight modifications. Briefly, total adipose tissue or isolated adipocytes were homogenized in lysis buffer and caspase-1 activity was measured by the addition of the caspase-1-specific peptide YVAD-AFC. Cleavage of the substrate by caspase-1 releases AFC that can subsequently be quantified using a fluorimeter. By comparing the fluorescence of AFC from an untreated sample with a sample treated with the specific caspase-1 inhibitor Pralnacasan, caspase-1 activity can be determined.

Isolation and Culturing of Primary Adipocytes and White Adipose Tissue Explants

Freshly isolated mouse epididymal adipose tissue was used for the isolation of adipocytes and stromal vascular cells. Minced adipose tissue was digested using collagenase (Sigma-Aldrich) at a concentration of 5 mg/ml dissolved in Dulbecco's modified Eagle's medium (DMEM). Tissues were incubated for 45 min at 37°C and were subsequently filtered through a 250 μM nylon mesh filter. After centrifugation, the floating cells were collected as adipocytes and the pelleted cells as stromal vascular cells. Stromal vascular cells were cultured and differentiated toward adipocytes using standard protocols. A similar protocol was applied for the isolation of human adipocytes and stromal vascular cells. For culturing of white adipose tissue explants, freshly isolated fat was minced and directly brought into culture using DMEM supplemented with 10% fetal calf serum. Human adipose tissue was obtained from patients undergoing reconstructive abdominal surgery after written informed consent.

Histology

Morphometry of individual fat cells was assessed using digital image analysis. Microscopic images were digitized in 24 bit RGB (specimen level pixel size 1.28 × 1.28 um^2). Recognition of fat cells was initially performed by applying a region-growing algorithm on manually indicated seed points, and minimum Feret diameter was calculated. Differences between groups were studied using one-way univariate Anova. Tukey HSD post-hoc testing was applied for multiple comparison testing.

RNA and DNA Isolation and qPCR Analysis

RNA from animal tissues was isolated using TRIzol reagent (Invitrogen) following the manufacturer's instructions. RNA was reverse transcribed using the iScript cDNA Synthesis Kit (Bio-Rad Laboratories BV, Veenendaal, The Netherlands). Real-time PCR was done with a Power Sybr Green PCR master mix (Applied Biosystems) using a 7300 Real-Time PCR System (Applied Biosystems). Melt curve analysis was included to assure a single PCR product was formed. Values were corrected using the housekeeping gene 36B4 or beta2-microglobulin (B2M). DNA was isolated from adipose tissue and mitochondrial DNA was quantified using primers to detect mitochondrial D loop. Results were corrected for the total amount of DNA within samples using primer sequences to detect LPL. Primer sequences are available upon request.

Immunoblot Analysis

Immunoblotting was carried out using an ECL system (Amersham Biosciences, Diegem, Belgium). Equal amounts of cell lysates as determined by Bio-Rad Protein Assay reagent (Bio-Rad Laboratories BV) were resolved by SDS/PAGE on a 12% polyacrylamide gel. Proteins were transferred using the iBLOT system (Invitrogen) following the manufacturer's instructions. The pAKT and AKT antibody (R&D Systems), caspase-1 antibody (Santa Cruz), and actin antibody (Sigma-Aldrich) were used at a dilution of 1:1000, and the membranes were incubated overnight at 4°C. The secondary antibodies were used at a dilution of 1:5000. All incubations were performed in 1× Tris-buffered saline (pH 7.5), with 0.1% Tween 20 and 5% dry milk. In the final washings, dry milk was removed from the solution.

Statistical Analysis

Statistical significant differences were calculated using a Student's t test. The cutoff for statistical significance was set at a p value of 0.05 or below.

SUPPLEMENTAL INFORMATION

Supplemental Information includes four figures and one table and can be found with this article online at doi:10.1016/j.cmet.2010.11.011.

ACKNOWLEDGMENTS

This project was supported by a grant from the Dutch Diabetes Research Foundation. M.G.N. was supported by a Vici Grant of the Netherlands Organization of Scientific Research.

Received: October 8, 2009
Revised: April 19, 2010
Accepted: October 1, 2010
Published: November 30, 2010

REFERENCES

Dumasy, V., Delhaye, M., Cotton, F., and Deviere, J. (2004). Fat malabsorption screening in chronic pancreatitis. Am. J. Gastroenterol. *99*, 1350–1354.

Guilherme, A., Virbasius, J.V., Puri, V., and Czech, M.P. (2008). Adipocyte dysfunctions linking obesity to insulin resistance and type 2 diabetes. Nat. Rev. Mol. Cell Biol. *9*, 367–377.

Gurcel, L., Abrami, L., Girardin, S., Tschopp, J., and van der Goot, F.G. (2006). Caspase-1 activation of lipid metabolic pathways in response to bacterial pore-forming toxins promotes cell survival. Cell *126*, 1135–1145.

Handschin, C., and Spiegelman, B.M. (2006). Peroxisome proliferator-activated receptor gamma coactivator 1 coactivators, energy homeostasis, and metabolism. Endocr. Rev. *27*, 728–735.

He, F., Doucet, J.A., and Stephens, J.M. (2008). Caspase-mediated degradation of PPARgamma proteins in adipocytes. Obesity *16*, 1735–1741.

Hotamisligil, G.S. (2006). Inflammation and metabolic disorders. Nature *444*, 860–867.

Jager, J., Gremeaux, T., Cormont, M., Le Marchand-Brustel, Y., and Tanti, J.F. (2007). Interleukin-1beta-induced insulin resistance in adipocytes through down-regulation of insulin receptor substrate-1 expression. Endocrinology *148*, 241–251.

Kadowaki, T., Yamauchi, T., Kubota, N., Hara, K., Ueki, K., and Tobe, K. (2006). Adiponectin and adiponectin receptors in insulin resistance, diabetes, and the metabolic syndrome. J. Clin. Invest. *116*, 1784–1792.

Kanneganti, T.D., Ozoren, N., Body-Malapel, M., Am, A., Park, J.H., Franchi, L., Whitfield, J., Barchet, W., Colonna, M., Vandenabeele, P., et al. (2006). Bacterial RNA and small antiviral compounds activate caspase-1 through cryopyrin/Nalp3. Nature *440*, 233–236.

Kanneganti, T.D., Lamkanfi, M., and Núñez, G. (2007). Intracellular NOD-like receptors in host defense and disease. Immunity *27*, 549–559.

Kim, M.S., Sweeney, T.R., Shigenaga, J.K., Chui, L.G., Moser, A., Grunfeld, C., and Feingold, K.R. (2007). Tumor necrosis factor and interleukin 1 decrease RXRalpha, PPARalpha, PPARgamma, LXRalpha, and the coactivators SRC-1, PGC-1alpha, and PGC-1beta in liver cells. Metabolism *56*, 267–279.

Lagathu, C., Yvan-Charvet, L., Bastard, J.P., Maachi, M., Quignard-Boulange, A., Capeau, J., and Caron, M. (2006). Long-term treatment with interleukin-1beta induces insulin resistance in murine and human adipocytes. Diabetologia *49*, 2162–2173.

Lago, F., Dieguez, C., Gomez-Reino, J., and Gualillo, O. (2007). Adipokines as emerging mediators of immune response and inflammation. Nat. Clin. Pract. Rheumatol. *3*, 716–724.

Lamkanfi, M., Kanneganti, T.D., Van, D.P., Vanden, B.T., Vanoverberghe, I., Vandekerckhove, J., Vandenabeele, P., Gevaert, K., and Nunez, G. (2008). Targeted peptide-centric proteomics reveals caspase-7 as a substrate of the caspase-1 inflammasomes. Mol. Cell Proteomics *7*, 2350–2363.

Larsen, C.M., Faulenbach, M., Vaag, A., Volund, A., Ehses, J.A., Seifert, B., Mandrup-Poulsen, T., and Donath, M.Y. (2007). Interleukin-1-receptor antagonist in type 2 diabetes mellitus. N. Engl. J. Med. *356*, 1517–1526.

Miyake, K., Ogawa, W., Matsumoto, M., Nakamura, T., Sakaue, H., and Kasuga, M. (2002). Hyperinsulinemia, glucose intolerance, and dyslipidemia induced by acute inhibition of phosphoinositide 3-kinase signaling in the liver. J. Clin. Invest. *110*, 1483–1491.

Mokdad, A.H., Bowman, B.A., Ford, E.S., Vinicor, F., Marks, J.S., and Koplan, J.P. (2001). The continuing epidemics of obesity and diabetes in the United States. JAMA *286*, 1195–1200.

Netea, M.G., Demacker, P.N., Kullberg, B.J., Boerman, O.C., Verschueren, I., Stalenhoef, A.F., and van der Meer, J.W. (1996). Low-density lipoprotein receptor-deficient mice are protected against lethal endotoxemia and severe gram-negative infections. J. Clin. Invest. *97*, 1366–1372.

Netea, M.G., Kullberg, B.J., Boerman, O.C., Verschueren, I., Dinarello, C.A., and Van der Meer, J.W. (1999). Soluble murine IL-1 receptor type I induces release of constitutive IL-1 alpha. J. Immunol. *162*, 4876–4881.

Netea, M.G., Joosten, L.A., Lewis, E., Jensen, D.R., Voshol, P.J., Kullberg, B.J., Tack, C.J., van Krieken, H., Kim, S.H., Stalenhoef, A.F., et al. (2006). Deficiency of interleukin-18 in mice leads to hyperphagia, obesity and insulin resistance. Nat. Med. *12*, 650–656.

Ntambi, J.M., Miyazaki, M., Stoehr, J.P., Lan, H., Kendziorski, C.M., Yandell, B.S., Song, Y., Cohen, P., Friedman, J.M., and Attie, A.D. (2002). Loss of stearoyl-CoA desaturase-1 function protects mice against adiposity. Proc. Natl. Acad. Sci. USA *99*, 11482–11486.

Ohara-Imaizumi, M., Cardozo, A.K., Kikuta, T., Eizirik, D.L., and Nagamatsu, S. (2004). The cytokine interleukin-1beta reduces the docking and fusion of insulin granules in pancreatic beta-cells, preferentially decreasing the first phase of exocytosis. J. Biol. Chem. *279*, 41271–41274.

Peronnet, F., and Massicotte, D. (1991). Table of nonprotein respiratory quotient: an update. Can. J. Sport Sci. *16*, 23–29.

Petrilli, V., Dostert, C., Muruve, D.A., and Tschopp, J. (2007). The inflammasome: a danger sensing complex triggering innate immunity. Curr. Opin. Immunol. *19*, 615–622.

Rudolphi, K., Gerwin, N., Verzijl, N., van der Kraan, P., and van den Berg, W. (2003). Pralnacasan, an inhibitor of interleukin-1beta converting enzyme,

reduces joint damage in two murine models of osteoarthritis. Osteoarthritis Cartilage *11*, 738–746.

Stienstra, R., Duval, C., Keshtkar, S., van der Laak, J., Kersten, S., and Muller, M. (2008). Peroxisome proliferator-activated receptor gamma activation promotes infiltration of alternatively activated macrophages into adipose tissue. J. Biol. Chem. *283*, 22620–22627.

van Rooijen, R.N., and Sanders, A. (1994). Liposome mediated depletion of macrophages: mechanism of action, preparation of liposomes and applications. J. Immunol. Methods *174*, 83–93.

Voshol, P.J., Jong, M.C., Dahlmans, V.E., Kratky, D., Levak-Frank, S., Zechner, R., Romijn, J.A., and Havekes, L.M. (2001). In muscle-specific lipoprotein lipase-overexpressing mice, muscle triglyceride content is increased without inhibition of insulin-stimulated whole-body and muscle-specific glucose uptake. Diabetes *50*, 2585–2590.

Wabitsch, M., Brenner, R.E., Melzner, I., Braun, M., Moller, P., Heinze, E., Debatin, K.M., and Hauner, H. (2001). Characterization of a human preadipocyte cell strain with high capacity for adipose differentiation. Int. J. Obes. Relat. Metab. Disord. *25*, 8–15.

Weisberg, S.P., McCann, D., Desai, M., Rosenbaum, M., Leibel, R.L., and Ferrante, A.W., Jr. (2003). Obesity is associated with macrophage accumulation in adipose tissue. J. Clin. Invest. *112*, 1796–1808.

Wilmanski, J.M., Petnicki-Ocwieja, T., and Kobayashi, K.S. (2008). NLR proteins: integral members of innate immunity and mediators of inflammatory diseases. J. Leukoc. Biol. *83*, 13–30.

Xu, H., Barnes, G.T., Yang, Q., Tan, G., Yang, D., Chou, C.J., Sole, J., Nichols, A., Ross, J.S., Tartaglia, L.A., and Chen, H. (2003). Chronic inflammation in fat plays a crucial role in the development of obesity-related insulin resistance. J. Clin. Invest. *112*, 1821–1830.

Zhou, R., Tardivel, A., Thorens, B., Choi, I., and Tschopp, J. (2010). Thioredoxin-interacting protein links oxidative stress to inflammasome activation. Nat. Immunol. *11*, 136–140.